

286 **Supplementary file: Detailed methodology**287 *Experiments*

288 Fluorite synthesis experiments were performed in a 40ml PFA reaction vessel at 60°C, with
289 temperature controlled by an externally heated waterbath and monitored by a teflon-sleeved
290 type-K thermocouple extended into the solution (Fig DR1). The vessel contained 30ml of a
291 starting solution consisting of 2.5 wt% CaCl₂, Ca(NO₃)₂ or CaSO₄ depending on the desired
292 dominating ligand, and 42 trace elements added at levels between 0.25 and 20 ppm (Table DR1).
293 The solution was prepared from >99.9% pure, single element chlorides, sulfates and nitrates
294 dissolved in nano-pure water. When hydrated chemicals were used, the mass fraction water
295 was determined by Thermo-Gravimetric Analysis (100mg of sample heated at 20Kmin⁻¹ up
296 to 350 °C followed by 1min isothermal in a quartz-glass holder using a DuPont TGA951,
297 resulting in a better than 5% reproducibility) and concentrations were adjusted accordingly.
298 Dissociation reactions, mainly involving TiCl₄, ZrOCl₂, HfOCl₂, SbCl₃ and BiCl₃, resulted in
299 the formation of a minor precipitate in the starting solution that was subsequently removed by
300 filtration, as well as a pH between 2.0 and 2.9. These compounds were not included in NO₃
301 experiments to minimize Cl-content, and trace element grade HNO₃ was added to generate the
302 same pH. The solution was stirred vigorously by a teflon-coated magnetic stirrer. At the run
303 temperature, 4ml of 1M CsF-solution was injected into the starting solution, causing fluorite
304 precipitation. The amount of F added represented a deficit relative to Ca to avoid precipitation
305 of other phases and a solid to liquid ratio of approximately 500. Experiments were subsequently
306 left for two hours at the run temperature, followed by recovery of fluorite and the reacted
307 solution by filtration through a 0.45µm filter. Cl and SO₄-solutions were clear after one
308 filtration, whereas NO₃-solutions required multiple filtration steps. Solid material was rinsed

309 repeatedly after filtration with nano-pure water.

310 *Characterization of run products*

311 An aliquot of solid run product was characterized by XRD at the Ceramics Research Centre,
312 Corus RD&T (the Netherlands) using a Bruker D4instrument. This showed that it consists of
313 well-developed crystalline mono-mineralic fluorite and can therefore be compositionally
314 characterized by a bulk technique. REE concentrations are high in the synthesized fluorite, but
315 do not reflect co-precipitation of REE-fluorides, because the characteristic peaks of these
316 fluorides are absent in the XRD spectra (Fig 2) Furthermore, REE concentrations in the final
317 solution do not increase with atomic mass and are therefore inconsistent with the solubilities
318 of the REE-fluorides (cf. Migdisov et al. 2009). The remaining material was digested using a
319 closed-vessel hot HNO₃-H₃BO₃ method (step 1: 50 mg fluorite + 0.25 ml concentrated HNO₃
320 + 1.5 ml of 2850 ppm H₃BO₃-solution in a teflon container at 90 °C for 10 minutes; step 2:
321 cooled and left to stand for 24 hours; step 3: 1.5ml of B-solution + 1.5ml 2% HNO₃ added and
322 heated to 90 °C for 4 hours; step 4: taken up in 2% HNO₃ to 10ml). The digested fluorite,
323 starting solutions and reacted solutions were analyzed by ICP-AES at Activation Laboratories
324 (Ancaster, Canada) for major elements and by ICP-MS at the Trace Element Analysis
325 Laboratory of McGill University for trace elements (detection limits of the analyses are given
326 in Table DR2). Partition coefficients were calculated from measured concentrations in fluorite-
327 solution pairs, supplemented with concentrations determined by mass-balance from the starting
328 solution composition where the concentration of an element in one of the end-products could
329 not be determined. The mass-balance method was also used as a check on the measured
330 concentrations. Partition coefficients show large variations in magnitude (Table DR1), as a result
331 of the low temperature of our experiments. This led to analytical challenges as the range of

332 concentrations exceeds the dynamic range of the ICP-MS. We therefore analyzed all samples
333 at a range of dilutions, providing us with multiple measurements for each element. This
334 approach also provides a means to check for enhancement and suppression matrix effects (none
335 were observed). Experiments involving Cl were conducted in double duplicate and reported
336 partition values are the average of these duplicates with associated 1 sigma experimental +
337 analytical uncertainty. For NO_3 and SO_4 experiments the propagated 2 sigma analytical
338 uncertainty is reported.

339 *Attainment of equilibrium*

340 A key concern for low temperature precipitation experiments is whether the results represent
341 equilibrium. We have several reasons to conclude that the partitioning we observe does reflect
342 equilibrium. Firstly, partition coefficients are highly reproducible as indicated by the four Cl-
343 bearing experiments. Furthermore, despite variations in the actual partition coefficients among
344 these experiments, the systematic differences among coefficients are identical and consistent
345 with lattice-strain control. Secondly, the observation of lattice-strain systematics in our
346 partitioning data is in itself strong evidence of equilibrium, as no such correspondence would
347 be observed if disequilibrium or other processes including absorption control trace element
348 concentrations. This is especially true for the diverse set of elements (in terms of radius and
349 charge) considered in our experiments and for the very large range of D-values obtained.
350 Thirdly, Ca concentrations in the fluid (10 to 8 ppm) are consistent with those expected from
351 fluorite solubility data (19.5 ppm- Richardson and Holland 1979; 13 ppm- Garand and Mucci
352 2004), indicating that the fluorite is in major-element equilibrium with its solution.

353 *Data fitting and speciation calculations*

354 Radii for the elements were taken from Shannon (1976) for a coordination number of 8, which
355 is the coordination of the single cation site in the fluorite structure. For elements for which 8-
356 coordinated radii were not listed, their radii were estimated using the systematic variations
357 among radius, coordination number and charge that were also employed by Shannon (1976).
358 All radii are given in Table DR1. Partition coefficients were fitted using the lattice-strain
359 equations of Blundy and Wood (1994) and fit parameters for the different experiments are
360 listed in Table DR3. The speciation at 60 °C, 1 bar and the composition of the experimental
361 solution was determined from thermodynamic calculations. Fluorite was the only solid phase
362 considered in the calculations. Thermodynamic properties for the aqueous species were taken
363 from the SupGrt database (http://geopig.asu.edu/supcrt92_data/slop98.dat) supplemented with
364 data for the REE (Migdisov et al. 2009) and Al (Tagirov and Schott 2001). Properties for
365 neutral F-species were estimated using the approach of Shock and Helgeson (1988) and
366 Sverjensky et al. (1997). Speciation-corrected partition coefficients were calculated by
367 dividing bulk coefficients by the fraction of each element residing in the species of interest.
368 Because thermodynamic data on aqueous species are limited, we had to combine all species
369 with a given ligand (see Table DR4).

370 *References*

371 Blundy, J. and Wood, B., 1994, Prediction of crystal-melt partition coefficients from elastic
372 moduli: *Nature* v. 372, p. 452-454.

373 Garand, A. and Mucci, A., 2004, The solubility of fluorite as a function of ionic strength and
374 solution composition at 25°C and 1 atm total pressure: *Marine Chemistry*, v. 91, p. 27– 35.

375 Migdisov, A.A., Williams-Jones, A.E. and Wagner, T., 2009, An experimental study of the
376 solubility and speciation of the Rare Earth Elements (III) in fluoride- and chloride-bearing
377 aqueous solutions at temperatures up to 300°C: *Geochimica et Cosmochimica Acta*, v. 73, p.
378 7087-7109.

379 Richardson, C.K. and Holland, H.D., 1979, The solubility of fluorite in hydrothermal solutions,
380 an experimental study: *Geochimica et Cosmochimica Acta*, v. 43, p. 1313–1325.

381 Shannon, R.D., 1976, Revised effective ionic radii and systematic studies of interatomic
382 distances in halides and chalcogenides: *Acta Crystallographica*, v. A32, p. 751-767.

383 Shock, E.L. and Helgeson, H.C., 1988, Calculation of the thermodynamic and transport
384 properties of aqueous species at high pressures and temperatures: Correlation algorithms for
385 ionic species and equation of state predictions to 5 kb and 1000 °C: *Geochimica et*
386 *Cosmochimica Acta*, v. 52, p. 2009-2036.

387 Sverjensky, D.A., Shock, E.L. and Helgeson, H.C., 1997, Prediction of the thermodynamic
388 properties of aqueous metal complexes to 1000 °C and 5 kb: *Geochimica et Cosmochimica*
389 *Acta*, v. 61, p. 1359-1412.

390 Tagirov, B. and Schott, J., 2001, Aluminum speciation in crustal fluids revisited: *Geochimica*
391 *et Cosmochimica Acta*, v. 65, p. 3965-3992.

392 *Figure and table captions*

393 Figure DR1

394 Schematic drawing of the experimental setup. Experiments were conducted by synthesizing
395 fluorite in an aqueous solution doped with 42 trace elements covering a wide range of radius
396 and charge. Effects of speciation were investigated by varying the dominant ligand of the
397 starting solution among Cl, NO₃ and SO₄. Experiments were conducted in a stirred teflon
398 reaction vessel within a thermostated waterbath at 60 °C. Fluorite precipitation was brought
399 about by injecting a 1M CsF-solution at run temperature.

400 Table DR1

401 Compositions of starting solutions of the various experiments (SSL) and the logarithm of
402 resulting partition coefficients between fluorite and aqueous solution. The charge of the
403 elements and their radius in 8-coordination are also given.

404 Table DR2

405 Analytical detection limits.

406 Table DR3

407 Lattice-strain fit parameters of the experimental partition coefficients.

408 Table DR4

409 Fraction of the elements residing as free ion (M), O or OH speciated (MOH), F-speciated (MF)
410 and Cl-speciated (MCl) as determined from thermodynamic modeling for the average
411 composition of final solutions of the FLU-4 series of experiments. Lack of data prevented us
412 from determining fractions for all elements.

H																	He
Li	Be											B	C	N	O	F	Ne
Na	Mg											Al	Si	P	S	Cl	Ar
K	Ca	Sc	Ti	V	Cr	Mn	Fe	Co	Ni	Cu	Zn	Ga	Ge	As	Se	Br	Kr
Rb	Sr	Y	Zr	Nb	Mo	Tc	Ru	Rh	Pd	Ag	Cd	In	Sn	Sb	Te	I	Xe
Cs	Ba	La	Hf	Ta	W	Re	Os	Ir	Pt	Au	Hg	Tl	Pb	Bi	Po	At	Rn
Fr	Ra	Ac															

La	Ce	Pr	Nd	Pm	Sm	Eu	Gd	Tb	Dy	Ho	Er	Tm	Yb	Lu
Ac	Th	Pa	U	Np	Pu	Am	Cm	Bk	Cf	Es	Fm	Md	No	Lr

1+ 20 ppm
2+ 5 ppm
3+ 0.25 ppm
4+ 5 ppm
 ligand elements and major cations
radius: ● 1 Å

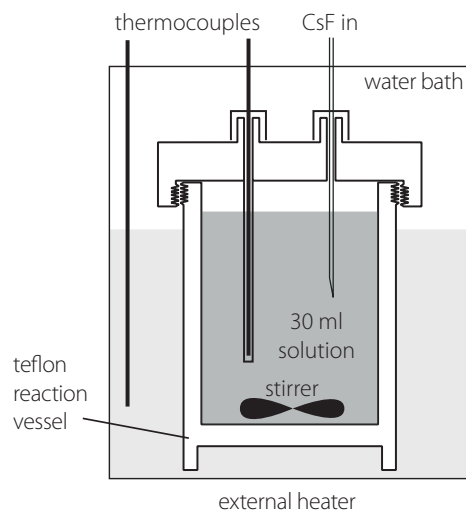


Figure DR1

Table DR1. Compositions of starting solutions of the various experiments (SSL) and the logarithm of resulting partition coefficients between fluorite and aqueous solution. The charge of the elements and their radius in 8-coordination are also given.

Experiment	FLU - 4					FLU - 6					FLU - 8					element props	
Ligand	Cl					NO ₃					SO ₄						
Temperature	60 °C					60 °C					60 °C						
Pressure	1 bar					1 bar					1 bar						
Element	SSL-4	FLU-4A	1 stdev		FLU-4B	1 stdev		SSL-6	FLU-6.1	2 stdev		SSL-8	FLU-8.2	2 stdev		radius	charge
	ppm	log D	-	+	log D	-	+	ppm	log D	-	+	ppm	log D	-	+	Å	
Li	20.47	1.34	0.10	0.08	1.40	0.19	0.13	21.65	1.42	0.15	0.11	14.82	0.95	0.08	0.07	0.920	1 +
Na	17.77	2.01	0.08	0.07	2.15	0.92	0.27	17.91	1.82	0.05	0.04	21.00	2.19	0.14	0.11	1.180	1 +
K	19.04	1.14	0.22	0.15	0.84	0.39	0.20	19.65	0.59	0.05	0.04	42.80	0.39	0.14	0.11	1.510	1 +
Rb	20.65	-0.27	0.08	0.07	-0.66	0.42	0.21	21.12	-1.30	0.07	0.06	15.30	0.05	0.26	0.16	1.610	1 +
Mg	5.19	2.68	0.20	0.14	2.69	1.12	0.28	5.51	2.22	0.20	0.14	7.05	2.01	0.02	0.02	0.890	2 +
Sr	5.07	3.70	0.22	0.14	4.14	-	0.33	6.49	2.56	0.11	0.09	3.64	2.16	0.01	0.01	1.260	2 +
Pb	4.72	3.44	0.32	0.18	4.58	0.01	0.01	5.21	2.88	-	0.33	3.92	1.96	0.02	0.02	1.290	2 +
Co	4.91	1.08	0.68	0.25	1.37	-	0.36	4.93	1.09	0.22	0.15	3.71	0.80	0.01	0.01	0.900	2 +
Ni	4.70	0.24	0.15	0.11	0.38	0.10	0.08	5.30	0.24	0.26	0.16	3.67	0.62	0.02	0.02	0.855	2 +
Cu	5.46	1.45	0.10	0.08	1.77	0.07	0.06	5.03	1.48	0.23	0.15	3.06	1.17	0.04	0.04	0.889	2 +
Zn	6.24	2.02	0.38	0.20	2.16	-	0.35	5.82	2.00	0.15	0.11	3.65	1.28	0.03	0.03	0.900	2 +
Mn	5.14	2.39	0.23	0.15	2.58	-	0.31	5.13	2.27	0.07	0.06	3.68	1.77	0.02	0.02	0.960	2 +
Fe	4.90	3.05	0.06	0.06	2.99	-	0.36	4.45	1.88	0.05	0.04	10.15	1.87	0.02	0.02	0.920	2 +
Sn	1.16	2.83	0.17	0.12	3.34	1.27	0.29	3.17	1.73	0.11	0.09	0.01	< d.l.f.	-	-	1.263	2 +
Al	4.64	< d.l.f.	-	-	2.57	1.18	0.29	4.36	4.87	0.05	0.04	10.34	2.51	0.03	0.02	0.649	3 +
Ga	14.31	4.06	0.20	0.13	4.53	0.42	0.21	18.78	3.64	-	0.79	11.26	1.94	0.01	0.01	0.736	3 +
Sc	4.88	5.41	0.35	0.19	5.69	0.12	0.09	n.p.	n.p.	-	-	5.08		0.02	0.02	0.870	3 +
Sb	0.06	1.97	0.33	0.18	2.74	-	0.32	n.p.	n.p.	-	-	0.01	0.95	0.06	0.05	0.879	3 +
Bi	0.05	3.88	0.01	0.01	4.42	-	0.35	n.p.	n.p.	-	-	6.29	2.14	0.02	0.02	1.170	3 +
Cr	5.36	1.60	0.52	0.23	1.70	-	0.37	5.15	0.21	-	1.87	4.50	0.40	0.01	0.01	0.731	3 +
Y	0.33	< d.l.f.	-	-	5.52	0.46	0.22	0.29	5.33	0.03	0.03	0.43	5.24	0.55	0.24	1.019	3 +
La	0.25	5.61	1.29	0.29	5.46	0.66	0.25	0.26	5.70	0.92	0.27	0.45	4.10	0.02	0.02	1.160	3 +
Ce	0.28	5.14	0.59	0.24	5.08	0.12	0.10	0.27	5.18	0.20	0.13	0.47	5.24	0.11	0.09	1.143	3 +
Nd	0.27	5.20	0.47	0.22	5.52	0.83	0.27	0.28	< d.l.f.	-	-	0.46	5.00	0.16	0.12	1.109	3 +
Sm	0.26	6.12	2.58	0.30	5.93	-	0.34	0.28	< d.l.f.	-	-	0.43	5.06	0.25	0.16	1.079	3 +
Eu	0.25	5.76	0.07	0.06	5.48	0.90	0.27	0.28	4.81	0.23	0.15	0.47	4.96	0.17	0.12	1.066	3 +
Gd	0.25	5.70	0.49	0.23	5.49	0.67	0.25	0.28	5.91	0.25	0.16	0.36	5.21	0.31	0.18	1.053	3 +
Tb	0.26	6.23	0.47	0.22	5.97	-	0.34	0.28	< d.l.f.	-	-	0.46	5.19	0.34	0.19	1.040	3 +
Dy	0.27	< d.l.f.	-	-	5.30	0.80	0.27	0.28	< d.l.f.	-	-	0.46	5.17	0.28	0.17	1.027	3 +
Ho	0.26	5.73	0.21	0.14	5.52	0.78	0.26	0.28	5.63	0.16	0.12	0.41	5.25	0.32	0.18	1.015	3 +
Er	0.26	< d.l.f.	-	-	5.48	0.66	0.25	0.28	< d.l.f.	-	-	0.47	5.18	0.51	0.23	1.004	3 +
Yb	0.27	5.91	0.53	0.23	5.64	1.37	0.29	0.27	6.11	0.25	0.16	0.44	5.28	0.54	0.23	0.985	3 +
Lu	0.27	< d.l.f.	-	-	5.23	0.83	0.27	0.27	< d.l.f.	-	-	0.47	5.31	0.50	0.23	0.977	3 +
Ti	4.22	3.14	0.07	0.06	3.81	0.18	0.13	n.p.	n.p.	-	-	3.15	< d.l.f.	-	-	0.740	4 +
Zr	2.43	4.46	0.21	0.14	4.37	-	0.37	n.p.	n.p.	-	-	2.24	3.54	0.06	0.06	0.840	4 +
Ge	3.64	2.08	0.53	0.23	2.11	-	0.35	n.p.	n.p.	-	-	0.83	0.97	0.03	0.03	0.669	4 +
Hf	4.77	4.45	0.02	0.02	4.57	0.02	0.02	n.p.	n.p.	-	-	4.12	3.34	0.05	0.04	0.830	4 +

Footnotes: n.p. not present in the starting solution, <d.l.f. below the limit of detection in the reacted solution, standard deviations are duplicate uncertainty for FLU-4A and 4B, and count statistical analytical error for FLU-6 and 8

Table DR2. Analytical
detection limits

Element	d.l (ppb)
Li	0.19
Na	100
K	100
Rb	0.008
Mg	2.59
Sr	0.048
Pb	0.067
Co	0.015
Ni	0.093
Cu	0.44
Zn	1.38
Mn	0.038
Fe	10
Sn	0.046
Al	100
Ga	0.014
Sc	0.17
Sb	0.004
Bi	0.006
Cr	0.20
Y	0.004
La	0.043
Ce	0.044
Nd	0.017
Sm	0.003
Eu	0.003
Gd	0.004
Tb	0.002
Dy	0.002
Ho	0.005
Er	0.003
Yb	0.002
Lu	0.002
Ti	0.09
Zr	0.012
Ge	0.12
Hf	0.006

Table DR3. Lattice-strain fit parameters of the experimental partition coefficients.

Experiment	FLU-4A	FLU-4B	FLU-4	FLU-6.1	FLU-8.2
1+ elements					
log D_0	2.02	2.15	2.09	1.84	2.24
E	16.0	18.8	17.4	15.5	23.0
r_0	1.20	1.20	1.20	1.14	1.23
2+ elements					
log D_0	4.63	4.85	4.76	3.92	3.70
E	90	85	95	90	90
r_0	1.14	1.15	1.14	1.13	1.12
3+ elements					
log D_0	6.14	5.78	6.00	5.78	5.26
E	104	80	92	110	110
r_0	1.00	1.02	1.01	1.05	1.02
4+ elements					
log D_0	5.31	5.34	5.32	n.a.	4.54
E	66	60	63	n.a.	66
r_0	1.00	1.00	1.00	n.a.	1.02

Table DR4. Fraction of the elements residing as free ion (M), O or OH speciated (MOH), F-speciated (MF) and Cl-speciated (MCl) as determined from thermodynamic modeling for the average composition of final solutions of the FLU-4 series of experiments. Lack of data prevented us from determining this for all elements.

Element	M	MOH	MF	MCl
Li	0.9991	0.0000	0.0002	0.0008
Na	0.9959	0.0000	0.0000	0.0041
K	0.9997	0.0000	0.0001	0.0001
Rb	0.9953	0.0000	0.0011	0.0036
Mg	0.9850	0.0000	0.0025	0.0125
Sr	0.9869	0.0000	0.0002	0.0129
Ba	0.9919	0.0000	0.0001	0.0080
Pb	0.6565	0.0000	0.0059	0.3376
Co	0.9464	0.0000	0.0011	0.0526
Ni	0.9967	0.0000	0.0014	0.0020
Cu	0.9568	0.0000	0.0031	0.0401
Zn	0.8657	0.0000	0.0013	0.1330
Cd	0.4590	0.0000	0.0006	0.5404
Mn	0.9746	0.0000	0.0008	0.0246
Fe	0.9855	0.0000	0.0026	0.0119
Sn	0.0000	0.0000	0.0002	0.0048
Al	0.0000	0.0000	1.0000	0.0000
La	0.5595	0.0000	0.4102	0.0303
Ce	0.4216	0.0000	0.5586	0.0198
Nd	0.4878	0.0000	0.4984	0.0139
Sm	0.3673	0.0000	0.6195	0.0132
Eu	0.2544	0.0000	0.7307	0.0149
Gd	0.3068	0.0000	0.6772	0.0160
Tb	0.2359	0.0000	0.7522	0.0119
Dy	0.2175	0.0000	0.7717	0.0109
Ho	0.2178	0.0000	0.7714	0.0108
Er	0.2153	0.0000	0.7728	0.0119
Yb	0.1886	0.0000	0.8012	0.0102
Lu	0.1790	0.0000	0.8109	0.0100